VIRGINIA TECH

Diversity Achieving OFDM Based MIMO

Author:
Don-Roberts EMENONYE

May 11, 2019

CONTENTS

LIST OF FIGURES

LIST OF TABLES

I. Introduction

Digital Communications is at the heart of wireless communications. This realization mandates prospective wireless engineers to have a full understanding of the intricacies of digital transceivers. In this correspondence, all the major blocks of a digital transceiver are designed. Specifically, this report details the design of different modular blocks in a digital transceiver and presents their performance evaluation under various conditions.

Secondly, most communication systems employ multiple transmit and multiple receiver architectures to improve reliability. Hence, the second part of this project aims to evaluate the performance of diversity achieving systems under various conditions.

Finally, the data rate needed by most systems means that there is a non zero probability of encountering a frequency selective channel. Therefore, the final part of this correspondence involves simulating a MIMO system equipped with orthogonal frequency division multiplexing.

II. Objective of This Project

The objectives of this project are three folds. They are

- Detail the design.
- Evaluate the bandwidth efficiency and the energy efficiency of the selected design.
- Evaluate its synchronization performance.

III. Theory and Function Descriptions

A. Transmitter Design

The transmitting module contains the following blocks:

- A channel encoder.
- Modulation block.
- Space Time Coding Block.
- OFDM transmitter on each antenna.

1) Channel Encoding: It is well known that standard modulation fails to achieve channel capacity. In order to drive rates, close to capacity, most digital communication systems make use of channel coding in addition to standard modulation techniques. Channel codes selectively introduce redundant information into the transmitted data stream so that a small number of symbol errors can be corrected after demodulation. In this correspondence, convolutional codes are used to provide improved reliability. Convolutional codes take a small number of input bits and produce a small number of output bits each time period.

Figure 3.1 depicts a rate 1/3 convolutional encoder that is used in this project.

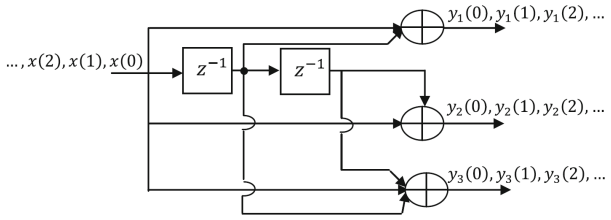

Fig. 1: A rate 1/3 linear convolutional encoder

The output streams will be represented as follows: y1(n) = x(n) + x(n-1); y2(n) = x(n) + x(n-2); y3(n) = x(n) + x(n-1) + x(n-2) The impulse response of this encoder can be represented as g1(n) = (110); g2(n) = (101); g3(n) = (111)

Table I shows the encoder properties used in this project.

SN	Properties	Value
1	Code rate	1/3
2	Constraint Length	3

TABLE I: Properties of the convolutional block employed

It should be noted that the convolutional encoder is implemented by convolving the input bits with the generator polynomials.

2) Modulation: Quadrature phase shift keying is the selected modulation scheme. It encodes two bits per symbol.

$$R_s = R_b/2 \tag{1}$$

It is selected based on the fact that it can achieve the same energy performance as binary phase shift keying, with an improvement in the spectral efficiency.

$$P_b = Q(\sqrt{\frac{E_s}{N_o}}) = Q(\sqrt{\frac{2E_b}{N_o}}) \tag{2}$$

Equation 2 details the energy performance of QPSK in an AWGN channel.

3) Space time coding - Diversity: This correspondence implements a 2 by 2 Alamouti scheme. At the transmitter space-time coding is implemented. Table II provides a brief definition of the space-time coding scheme.

Transmit time	Antenna 1	Antenna 2
t	s_1	s_2
$t + T_s$	$-s_2^*$	s_1^*

TABLE II: Alamouti space-time coding.

At some instant in time, t, symbol s_1 is transmitted from transmit antenna 1 and symbol s_2 is transmitted from the second transmit antenna. During the next symbol interval period at time t+Ts, the symbols $-s_2^*$ and s_1^* are transmitted from antennas 1 and 2, respectively. This demonstrates how Alamouti coding takes advantage of the spatial and temporal dimensions.

4) Orthogonal Frequency Division Multiplexing: The large bandwidth requirement of most systems indicates that the channel has a non-zero probability of being frequency selective. In order to combat the impact of a frequency selective channel, this project implements OFDM.

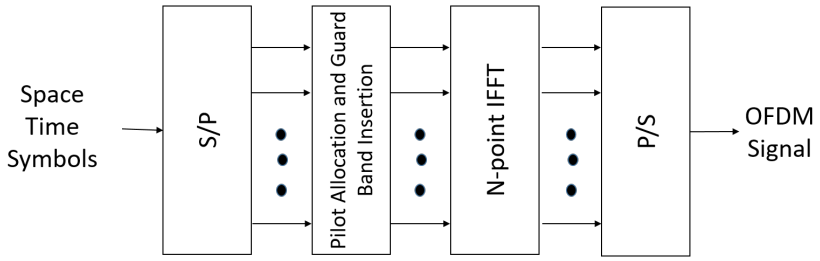

Fig. 2: Outline of OFDM Transmission

In this correspondence, OFDM is employed to divide the wide bandwidth of the signal into narrower orthogonal subcarriers.

TABLE III: Properties of OFDM Block

OFDM Parameters	Value
Number of Sub Carriers	128
Length of Cyclic Prefix	32
Length of Guard Carriers	8
Number of Data Sub carriers	96
Number of Pilot Sub Carriers	24

Table III depicts the OFDM properties employed in this project. It should be noted that OFDM is employed separately on each antenna

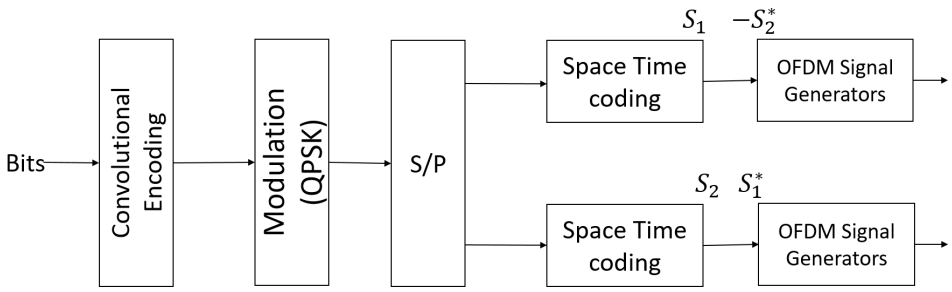

Fig. 3: Overall Transmitter Schematic

B. Receiver Design

The receive processing is done in two stages. They are: 1) the antenna specific processing and 2) the general processing. The following are procedures carried out at each receive antenna :

- Cyclic prefix based time synchronization.
- Removal of cyclic prefix and conversion to frequency domain (FFT).
- Channel estimation

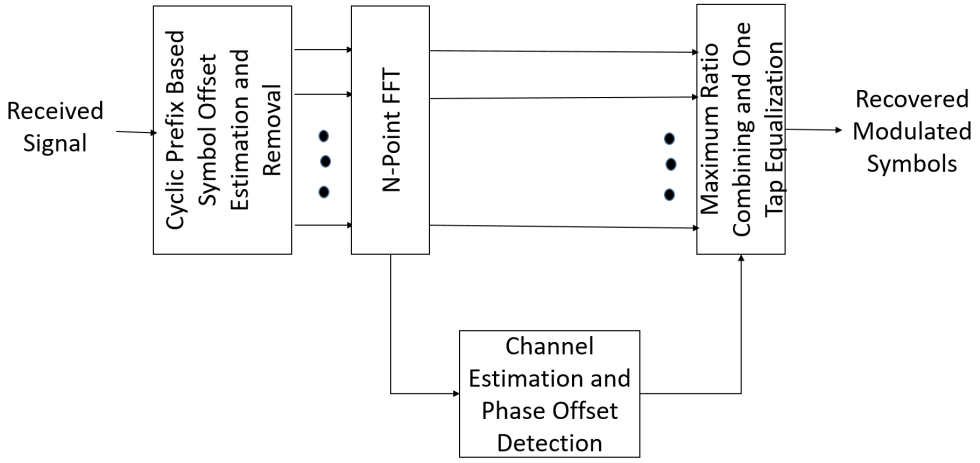

Fig. 4: First stage receiver operations

1) Cyclic Prefix Based Time Synchronization: In order to take the N-point FFT at each receiver, we need the exact samples of the transmitted signal for the OFDM symbol duration. In other words, symbol-timing synchronization must be performed to detect the starting point of each OFDM symbol, which facilitates obtaining the exact samples [1].

Recall that the cyclic prefix is a replica of a part of the OFDM signal. Hence, the CP and its corresponding location in the signal will share similarities which can be used for symbol timing estimation.

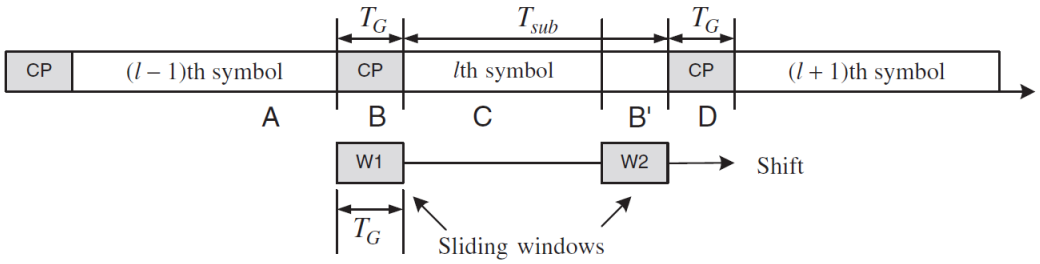

Fig. 5: Symbol Timing Estimation using double sliding windows[1]

Figure 5 denotes N_G samples of CP and another N_G samples of the data part by B and $B^{'}$ respectively. The windows W1 and W2 can slide to find the similarity between the two blocks of N_G . The similarity between two blocks of N_G samples in W1 and W2 is maximized when CP of an OFDM symbol falls into its corresponding data location. In fact, this maximum point can be used to identify the symbol time offset [1].

The similarity between the two blocks is maximized when the difference between them is minimized.

$$\hat{\delta} = \arg\min_{\delta} \sum_{i=\delta}^{N_G-1+\delta} (\mid y_l[n+i] \mid - \mid y_l^*[n+i+N] \mid)^2 \tag{3}$$

The symbol timing offset - δ - is calculated using equation 3.

2) Removal of cyclic prefix and conversion to frequency domain (FFT): At this stage, the cyclic prefix is removed. The ofdm symbols are then converted back to the frequency domain using a fast fourier transform.

3) Channel Estimation: In order to properly estimate the effects of the channel, pilots symbols are placed intelligently on different sub carriers in the ofdm symbol. In this correspondence, pilots are spaced apart by five sub carriers. The channel of the other sub carriers is gotten by interpolation. A vector of received pilots is shown in equation (4)

$$\boldsymbol{y} = \boldsymbol{h}\boldsymbol{x} + \boldsymbol{n} \tag{4}$$

The channel can be estimated by using:

$$\hat{\boldsymbol{h}} = \frac{\boldsymbol{y}^{\boldsymbol{H}}\boldsymbol{x}}{\|\boldsymbol{x}\|^2} \tag{5}$$

The conjugate of $\hat{\boldsymbol{h}}$ gives the estimated channel. **The channel estimation employed in this correspondence corrects any phase offsets**.

4) Maximum Ratio Combining: In this correspondence two antennas are used, the received signal on each antenna at time t and time $t + T_s$ is shown in equation 6.

$$\begin{aligned} r_1(1) &= r_1(t) = h_{11}s_1 + h_{12}s_2 + z_1(1) \\ r_1(2) &= r_1(t+T_s) = -h_{11}s_2^* + h_{12}s_1^* + z_1(2) \\ r_2(1) &= r_2(t) = h_{21}s_1 + h_{22}s_2 + z_2(1) \\ r_2(2) &= r_2(t+T_S) = -h_{21}s_2^* + h_{22}s_1^* + z_2(2) \end{aligned} \tag{6}$$

The received signals are combined as shown in equation 7

$$\begin{aligned} \tilde{s_1} &= h_{11}^* r_1(1) + h_{12} r_1^*(2) + h_{21}^* r_2(1) + h_{22} r_2^*(2) \\ \tilde{s_2} &= h_{12}^* r_1(1) - h_{11} r_1^*(2) + h_{22}^* r_2(1) - h_{21} r_2^*(2) \end{aligned} \tag{7}$$

$$\begin{aligned} \tilde{s_1} &= (\sum_{i=1}^{2}\sum_{j=1}^{2} \mid h_{ij} \mid^2) s_1 + h_{11}^* z_1(1) + h_{12} z_1^*(2) + h_{21}^* z_2(1) + h_{22} z_2^*(2) \\ \tilde{s_2} &= (\sum_{i=1}^{2}\sum_{j=1}^{2} \mid h_{ij} \mid^2) s_2 + h_{12}^* z_1^*(1) - h_{11}^* z_1^*(2) + h_{22}^* z_2^*(1) - h_{21}^* z_2^*(2) \end{aligned} \tag{8}$$

The remainder of the receive processing is not antenna specific and they are:

- MAP symbol estimation.
- Viterbi decoding.

5) MAP symbol estimation: It is quite clear to see that the combined signals in equation (8) takes the form given by equation (9).

$$\tilde{s} = ks + z \tag{9}$$

This realization implies that $\tilde{s}$ can be estimated using the MAP decision rule.

$$\hat{s} = \arg\max_{s} P(s|\tilde{s}) \tag{10}$$

Assuming equal likely symbols are sent, equation (10) is equivalent to (11)

$$\hat{s} = \arg\max_{s} P(\tilde{s}|s) \tag{11}$$

It is intuitive to see that the pdf of the combined symbol is centered at ks. Hence, equation (11) can be written as

$$\arg\min_{s} \mid \tilde{s} - ks \mid \tag{12}$$

The ML detection rule can be rewritten as

$$\begin{aligned} &\arg\min_{s}[(\tilde{s} - ks)(\tilde{s} - ks)^*] \\ &\arg\min_{s}[(k-1) \mid s \mid^2 + \mid \tilde{s} - s \mid^2] \end{aligned} \tag{13}$$

where k is equal to $\sum_{i=1}^{2}\sum_{j=1}^{2} \mid h_{ij} \mid^2$

$$\hat{s} = \arg\min_{s}[((\sum_{i=1}^{2}\sum_{j=1}^{2} \mid h_{ij} \mid^2) - 1) \mid s \mid^2 + \mid \tilde{s} - s \mid^2] \tag{14}$$

[5] provides a closed form expression of the bit error rate for a system employing QPSK, gray coding and Alamouti diversity.

$$p_b = \frac{1}{2}[1 - \frac{\mu}{\sqrt{2-\mu}} \sum_{k=0}^{L-1} \binom{2k}{k} (\frac{1-\mu^2}{4-2\mu^2})^k] \tag{15}$$

where μ is the snr associated with each diversity link and L is the diversity order.

6) Decoder: An encoder with m registers has 2^m possible states. The corresponding state diagram for the encoding employed in this correspondence is shown below.

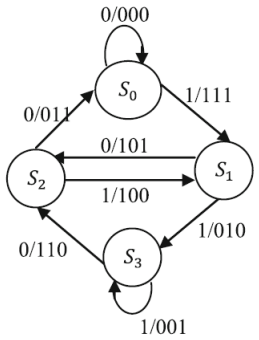

Fig. 6: State Diagram

While the state diagram details the input bits that leads to certain transitions, it does not contain the time information required in decoding. Hence, trellis diagrams are developed in order to overcome this disadvantage. The trellis diagram is an expansion of state diagram by adding a time axis for time information.

In this project, a $(3, 1)$ convolutional encoder with 2 registers is used, hence there are 2^2 nodes at each time instant. It is intuitive to see that the number of paths increases exponential with the length of the input bit sequence.

The Viterbi [3] algorithm is chosen to over come this disadvantage. The viterbi algorithm finds the best code sequence per stage as opposed to searching through all the possible code sequence.

IV. Performance Evaluation

The following channel test cases will be evaluated:

- Additive white Gaussian channel.
- Flat Rayleigh channel.
- Frequency selective Rayleigh channel

A. *Additive white Gaussian channel*

In order to develop a proper yard stick for comparison, it is necessary to start any performance evaluation using an AWGN channel.

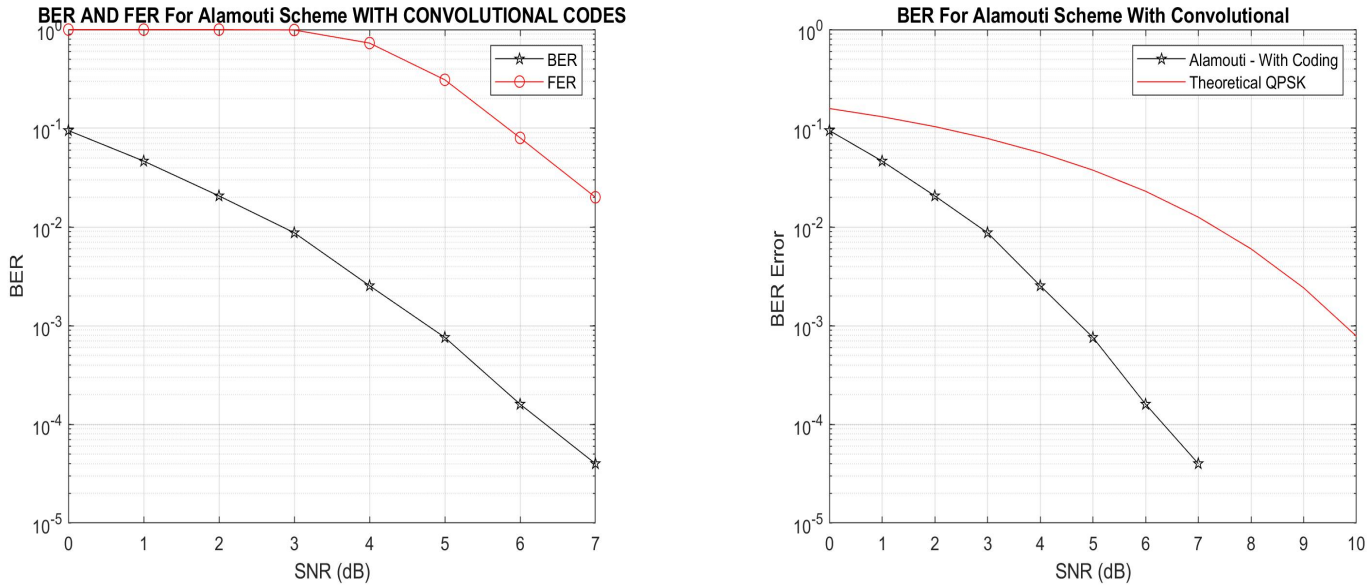

(a) BER AND FER For Designed Scheme in An AWGN Channel

(b) Theoretical Single Antenna VS Designed System

Fig. 7: Designed System Vs Single Antenna Transmission Under AWGN

The energy performance of the designed system is shown in Figure 8. Although there is no multi path in an AWGN channel, the designed scheme provides about 5dB improvement at high SNRs. This can be attributed to the fact that multiple copies of the same transmit symbols are obtained at each receiver due to combining.

B. *Flat Fading Channel*

Although, diversity can improve performance in an AWGN system by simply providing multiple copies of the same transmit symbol, the benefits of diversity are more prominent in fading channels.

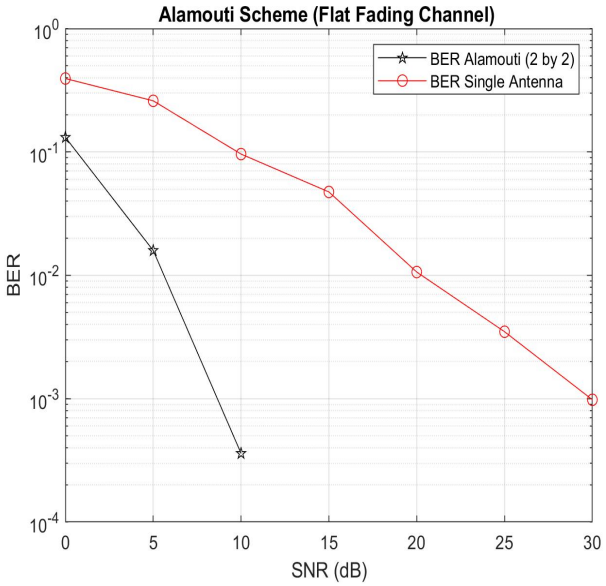

(a) Designed System VS Single Antenna

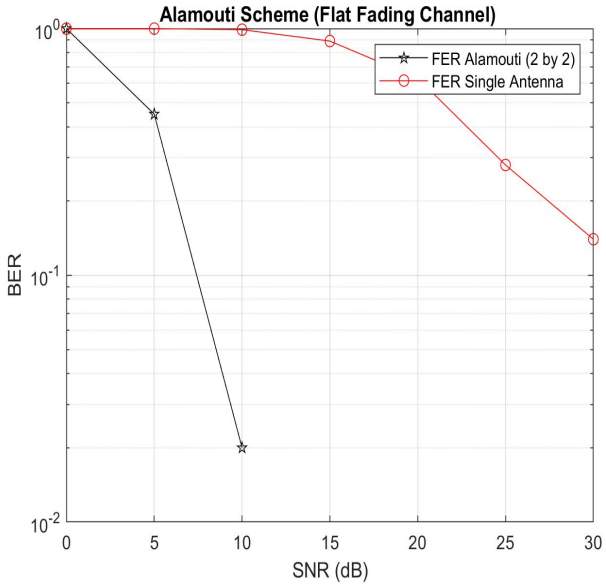

(b) Designed System Vs Single Antenna

Fig. 8: Designed System Vs Single Antenna Under Flat Fading Conditions

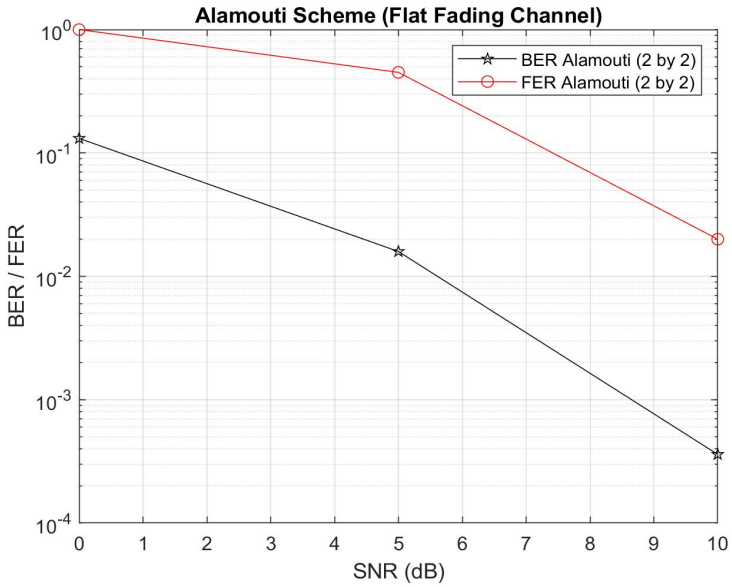

Fig. 9: BER And FER for The Designed System Under Flat Fading

C. *Frequency Selective Fading Channel*

This section analyzes the performance of the designed system under frequency selective conditions. The channel has four taps - [1, 0.15, 0.05, 0.01]. Also, the doppler spread is varied to induce fast varying channel conditions. OFDM is employed to ensure simplicity during equalization.

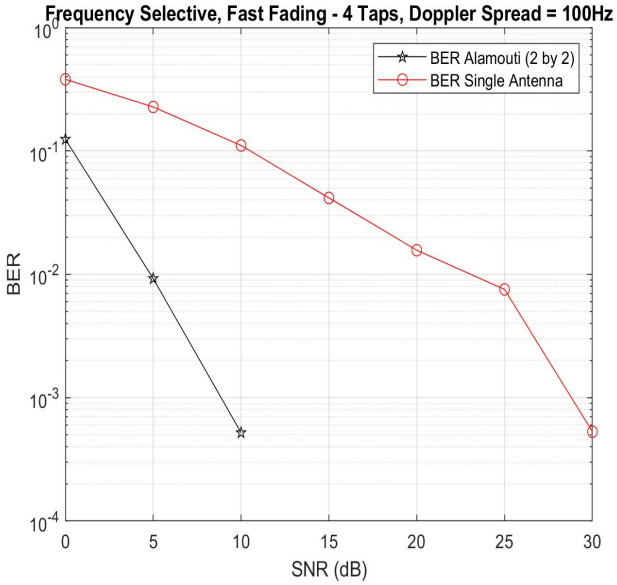

(a) Designed Scheme VS Single Antenna

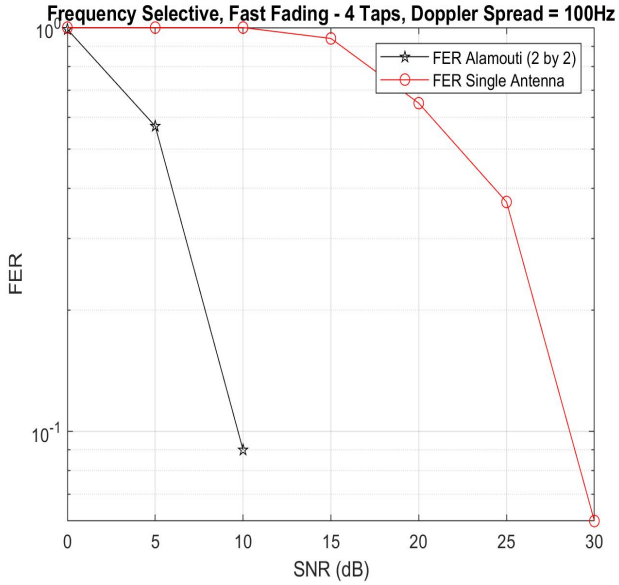

(b) Designed Scheme Vs Single Antenna

Fig. 10: Designed System Vs Single Antenna Under Frequecy Selective Conditions

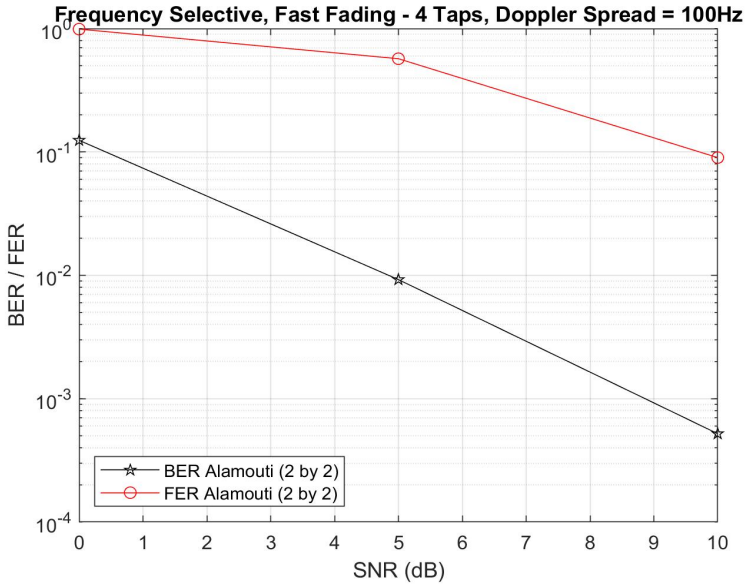

Fig. 11: BER And FER for The Designed System Under Frequency Selective Fading Conditions

Next, the doppler spread is increased to 1KHz, and the energy performance is simulated.

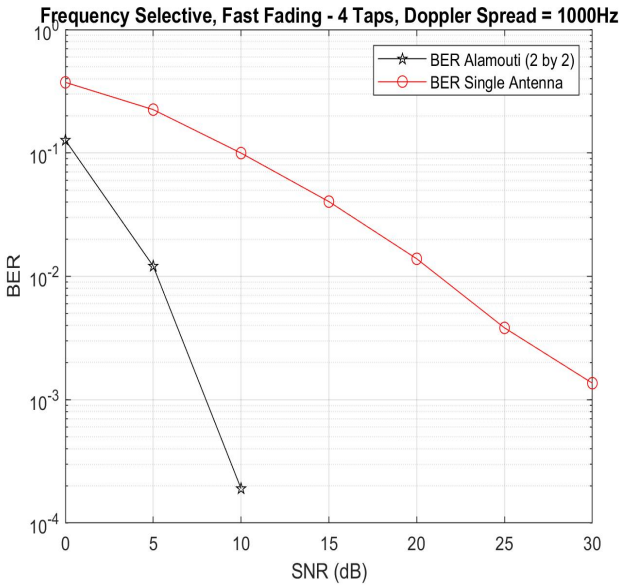

(a) Designed Scheme VS Single Antenna

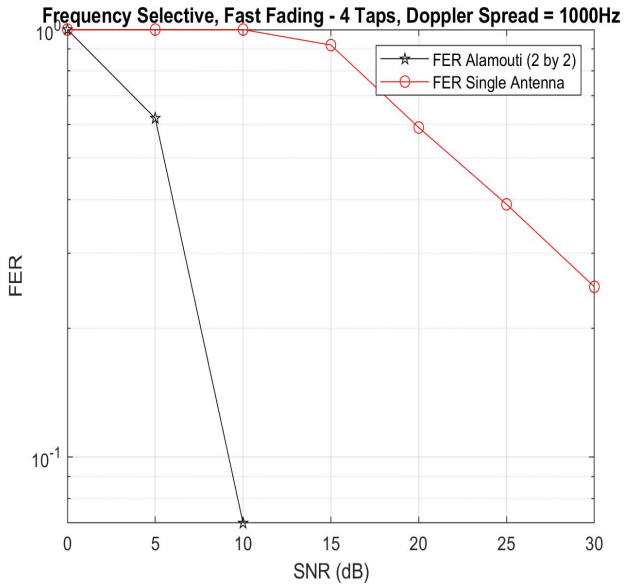

(b) Designed Scheme Vs Single Antenna

Fig. 12: Designed System Vs Single Antenna Under Frequency Selective and Fast Fading Conditions

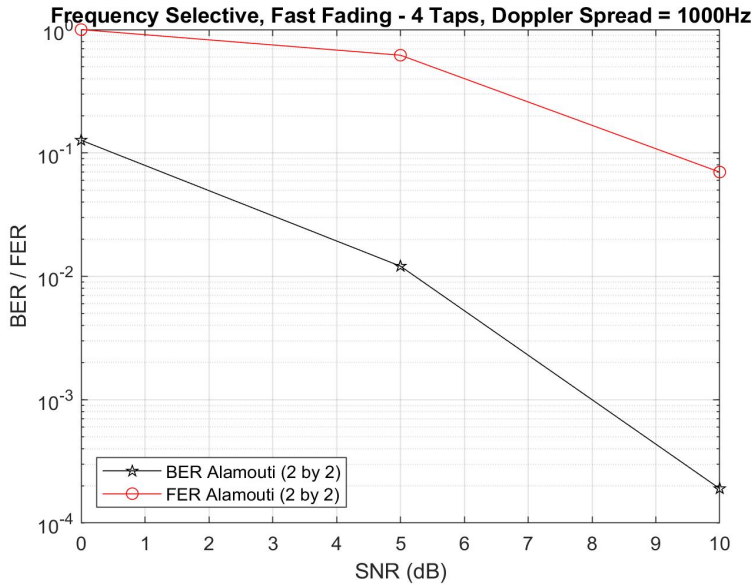

Fig. 13: BER And FER for The Designed System Under Frequency Selective and Fast Fading Conditions

D. Inference From Performance Plots

The following observations are evident from the comparison of the designed system with a single antenna scenario:

- The Alamouti scheme performs well in all the simulated channel test cases. This can be attributed to the fact that OFDM and single tap equalization are implemented in the frequency selective channel scenario.

- The bit error rate of the designed Alamouti scheme is significantly better than the single antenna scenario.

- At high SNR, the performance gains are more noticeable, this can be attributed to the maximum ratio combining used at the receivers.

E. Synchronization Performance Under AWGN

This section provides an evaluation of the system performance under timing and phase offset.

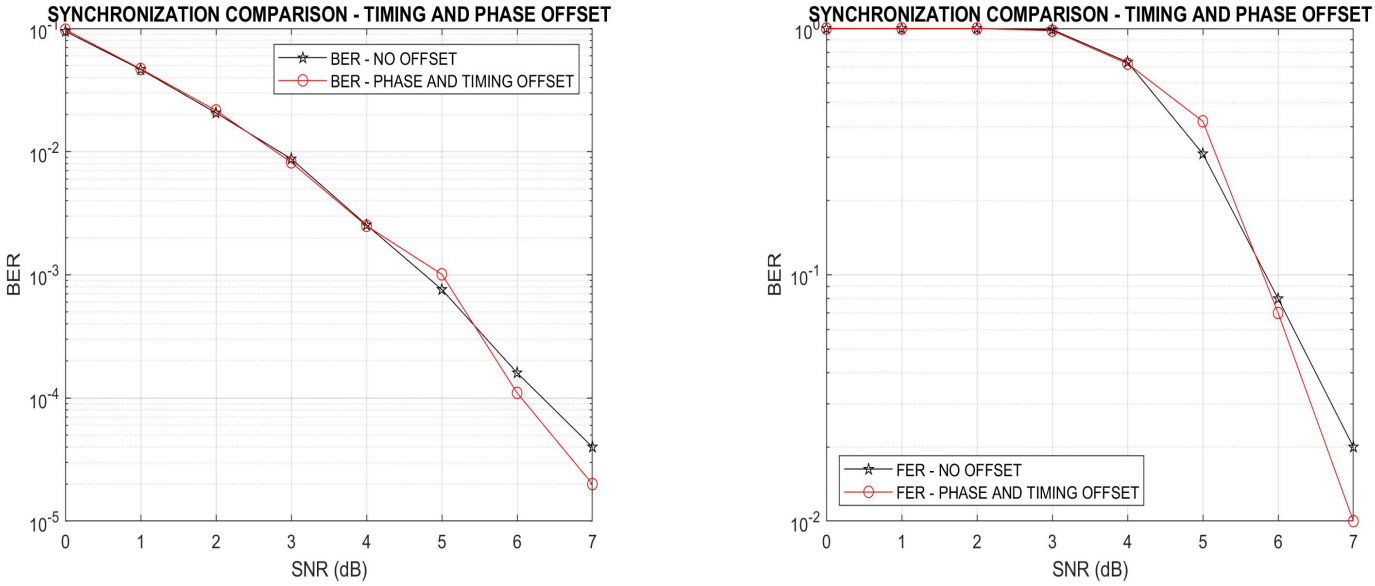

(a) Bit Error Rate Evaluation

(b) Frame Error Rate Evaluation

Fig. 14: Performance in the presence of Phase and Timing Offset

F. Synchronization Performance Under Flat Fading

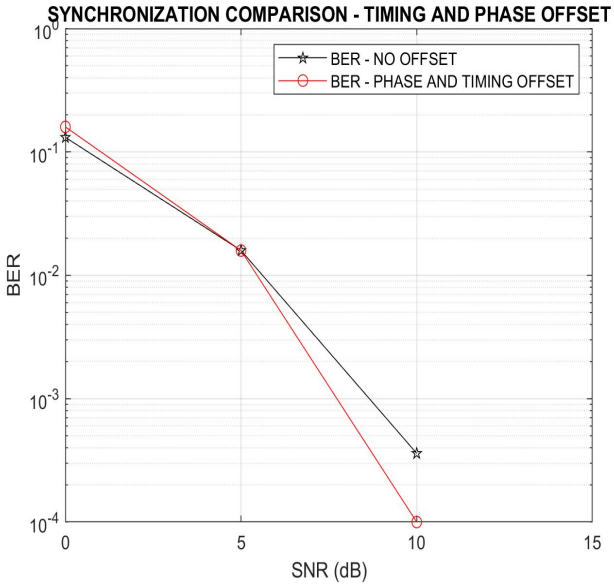

(a) Bit Error Rate Evaluation

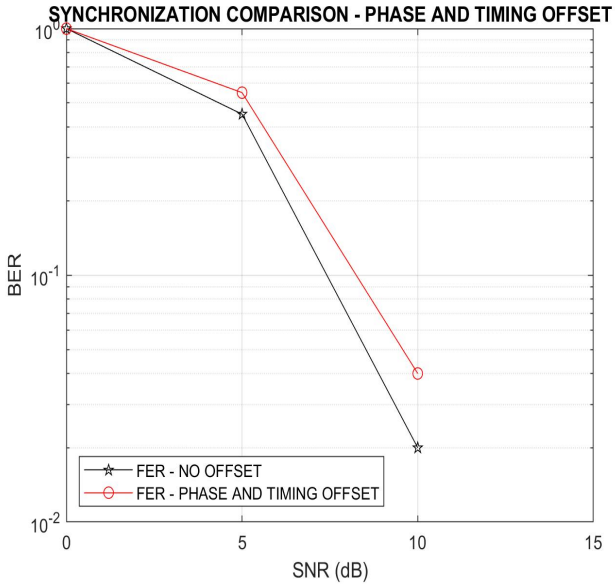

(b) Frame Error Rate Evaluation

Fig. 15: Performance in the presence of Phase and Timing Offset under flat fading

G. Synchronization Performance Under Frequency Selective Fading

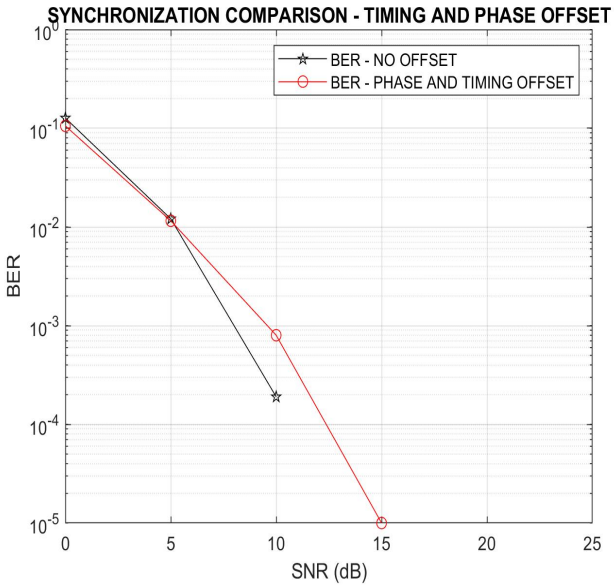

(a) Bit Error Rate Evaluation

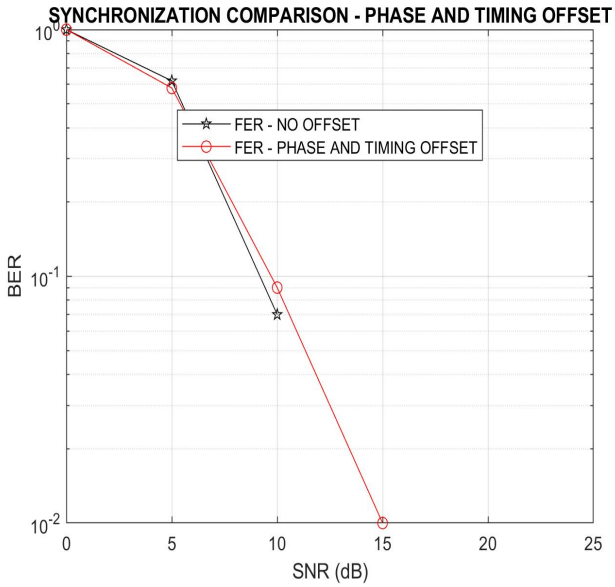

(b) Frame Error Rate Evaluation

Fig. 16: Performance in the presence of Phase and Timing Offset under frequency selective fading

From the above figures, it is clear that the designed system correctly offsets the effects of either timing, phase offset or both. However, this system fails to correct frequency offsets.

H. Inference From Synchronization Evaluation

The previous plots were generated by adding offsets after the effects of the channel and Gaussian noise. From figures 14, 15, and 16, it is evident that the designed system accurately corrects both timing and phase offsets. However, this OFDM-based system fails to correct any frequency offsets.

Figure 17 shows a degradation in energy performance due to the presence of a frequency offset in the MIMO OFDM system.

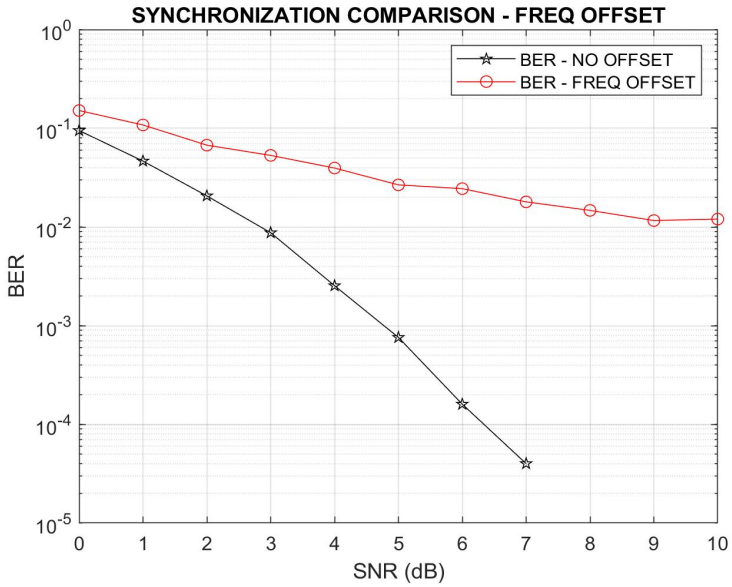

Fig. 17: Degradation of BER due to frequency offset in the MIMO OFDM system

I. Spectral Analysis

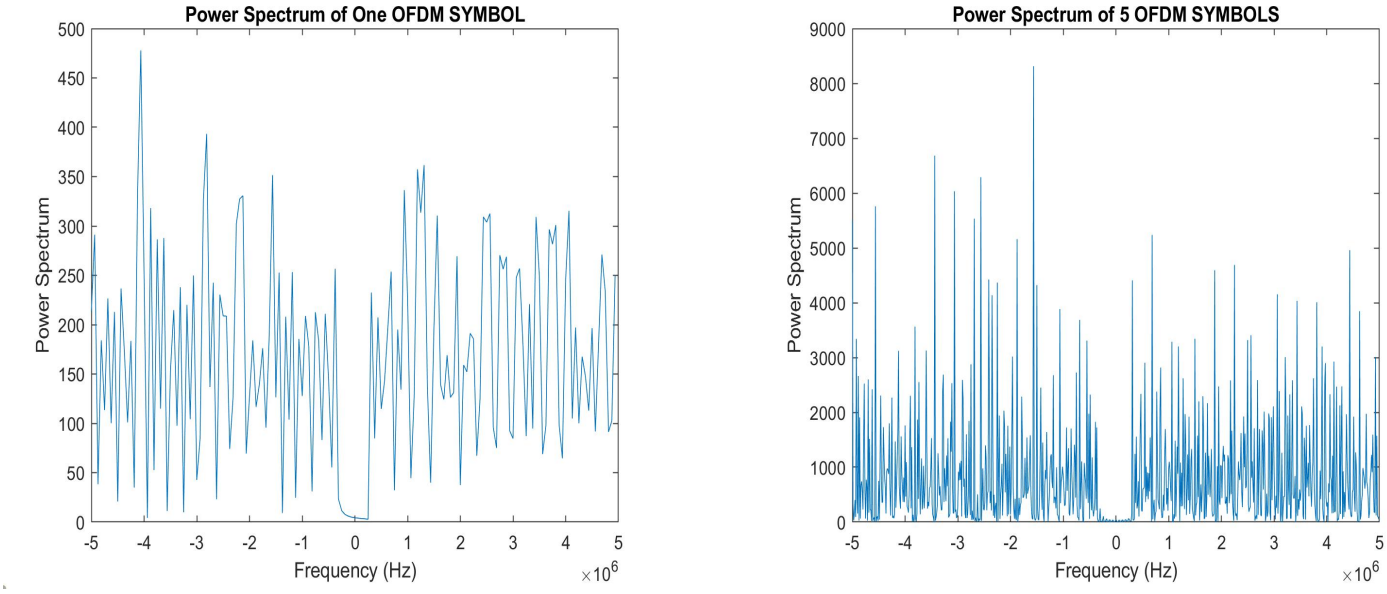

(a) Spectrum of the first OFDM Symbol

(b) Spectrum of first Five OFDM symbols

Fig. 18: Power Spectrum

This correspondence employs a rate (1/3) code and QPSK is the modulation scheme of choice. Hence, if we assume that the bandwidth equals the output sample rate, the theoretical bandwidth efficiency can be calculated as

$$\eta = \frac{R_b}{R_p} = \frac{R_b}{\frac{3}{2}R_b} = 0.6667 \tag{16}$$

Where R_p is the output sample rate and it equals $\frac{3\times R_b}{2}$. To get the actual bandwidth statistics, it is important to note that zero padding is employed in some modules. Hence, if we assume an output sample rate (R_p) of 10^7, the actual data rate can be calculated using

$$R_b = \frac{N_b \times R_s}{Ns} \tag{17}$$

where N_b is the number of input bits, and N_s is the number of output bits used for transmission.

In this design, a thousand bits was sent in one frame, but 5120 bits was produced by the transmitter, hence the data rate for a 10MHz bandwidth equals

$$R_b = 1.95Mb/s \tag{18}$$

V. General Observations

- A surprising observation is, the system uses the same bandwidth as the single antenna case. This occurs, because one symbol is still being transmitted during every symbol duration.
- An important observation is that the system only requires channel state information at the receiver (CSIR). Perhaps, this is the most important advantage of using this scheme.
- The equalization used in this scheme is tremendously straight forward, this is because orthogonal frequency division multiplexing is employed. The OFDM scheme reduces the equalization block to a simple one tap equalizer.
- The channel estimation and equalization corrects phase offsets.
- The optimal Alamouti decoder has a surprisingly low complexity - it is simply maximum ratio combining.

VI. Important Points To Note

- **All the plots were generated using 1000 bits in 100 frames, please use this parameters if convenient.**
- **There is an inflexible region of operation, equal timing offset must be added to both antennas**.
- Sadly, this system fails to correct frequency offsets. I tried a cyclic prefix based frequency offset estimation and it failed. Subsequently, I tried implementing the estimation in the frequency domain. I tested the Moose approach [4] and the Classen approach [2]. All the frequency techniques seem to detect offsets, when there was none. Hence, I had to completely remove it, so it won't ruin the other results.
- A trivial point to note is that my frequency estimation module worked without OFDM, but failed after OFDM was implemented.
- During the first run, coding parameters such as the distance between two states and the transition parameters are generated and stored in a .mat file.

VII. Conclusions

- The designed system provides a tremendous gain in energy efficiency without requiring either channel state information at the transmitter or a bandwidth expansion.
- The system maintains the same performance, even in frequency selective and fast fading channels. This is attributed to OFDM and single tap equalization.
- The system maintains approximately the same performance in the presence of timing and phase offsets.

REFERENCES

[1] Yong Soo Cho, Jaekwon Kim, Won Y Yang, and Chung G Kang. *MIMO-OFDM wireless communications with MATLAB*. John Wiley & Sons, 2010.

[2] Ferdinand Classen and Heinrich Meyr. Frequency synchronization algorithms for ofdm systems suitable for communication over frequency selective fading channels. In *Proceedings of IEEE Vehicular Technology Conference (VTC)*, pages 1655–1659. IEEE, 1994.

[3] G David Forney. The viterbi algorithm. *Proceedings of the IEEE*, 61(3):268–278, 1973.

[4] Paul H Moose. A technique for orthogonal frequency division multiplexing frequency offset correction. *IEEE Transactions on communications*, 42(10):2908–2914, 1994.

[5] John Proakis. *Masoud Salehi Digital Communications*. McGraw-Hill, 2008.